Quantum interference in carbon nanotube electron resonators

Linfeng Yang,[1,2] Jiangwei Chen,[1] Huatong Yang,[1] and Jinming Dong[1]
[1]*National Laboratory of Solid State Microstructures and Department of Physics, Nanjing University, Nanjing 210093, China*
[2]*Zhongyuan Institute of Technology, Zhengzhou 450007, China*

(Received 23 October 2003; revised manuscript received 6 January 2004; published 16 April 2004)

The quantum conductance fluctuations of the electron resonator composed of the single-walled carbon nanotube (SWNT) has been studied numerically. It is shown that the conductance oscillations appear at the strong coupling between the electrical contact and SWNT, and become well-defined resonant peaks as the coupling is very weak. It is also found that the disorder and defects in the SWNT cannot induce the observed slow and fast conductance oscillations. More importantly, it is demonstrated that the experimentally observed deep dip in the conductance G vs Fermi-energy plot is probably caused by the chemisorbed atoms on the SWNT.

DOI: 10.1103/PhysRevB.69.153407 PACS number(s): 73.22.−f, 73.23.−b, 73.63.Fg

The behavior of traditional electronic devices can be usually understood in terms of the classical diffusive electron motion. However, as the size of a device continuously decreases and becomes comparable to the electron coherence length, the quantum interference between electron waves becomes increasingly important, leading to dramatic changes in the device properties. This classical-to-quantum transition in the device behavior suggests the possibility of using quantum coherence in the nanometer-sized electronic elements. Molecular electronic devices are promising candidates of realizing such devices because the electronic motion in them is inherently quantum mechanical and can be modified by well-defined chemistry. Another example of the coherent electronic device is the Fabry-Perot electron resonator based on individual single-walled carbon nanotube (SWNT) with near-perfect ohmic contacts to electrodes,[1,2] in which the nanotube acts as a coherent electron waveguide with a resonant cavity formed between the two nanotube-electrode interfaces.

Within the Landauer formalism, the ballistic conductance of a perfect system is proportional to the number of conducting channels at the Fermi energy. In the case of an isolated metallic SWNT, there are two bands derived from the π-bonding and π-antibonding orbitals between neighboring carbon atoms, which cross at the Fermi level E_F, leading to a perfect transmission in the case of ideal electrical contact, and thus two units of quantum conductance $G=2G_0(G_0=2e^2/h)$. If the electrical contacts are imperfect, the elastic scattering on the interfaces affects the transmission coefficients and thereby reduces the conductance, which then is no longer precisely quantized. For SWNT's, the conductance $G=T(2G_0)=4Te^2/h$ with transmission probability up to $T\sim 0.5$–0.95 has been observed in the transport measurements.[2–5] In addition, the rapid conductance oscillations are observed to be superimposed on a slow fluctuation background, and several independent samples are observed to exhibit a deep dip in G vs gate voltage V_g. The fast conductance oscillations have been ascribed to the confinement-induced discrete ''particle-in-box'' electronic states, and both the slow oscillations and the dip to the localized states induced by defects. Recently, Jiang *et al.* have derived an analytical expression and successfully explained the main experimental results, showing that both rapid and slow conductance fluctuations are caused by the intrinsic quantum interference.[6] However, appearance of a deep dip in the conductance oscillations vs the gate voltage plot has not been solved until now. Also, the effects of different defects and disorders in the SWNT on both fast and slow conductance oscillations are an interesting problem, and have not been considered in the analytical expression. In this paper, we have numerically calculated the quantum conductance of the SWNT's with near transparent contacts by using a tight-binding-based Green's-function approach,[7] which easily includes the disorder effects, and the effect of contact coupling is also discussed. Our numerical calculations demonstrate that the conductance oscillations appear at the strong coupling between the electrical contact and SWNT, and become well-defined resonant peaks as the coupling is very weak. The disorders or topological defects in the SWNT cannot cause the slow conductance fluctuations, and on the contrary, the disorders will smear them. It is also found that the dip in the conductance curve is probably induced by the chemisorbed atoms on the SWNT, providing a consistent explanation for the observed phenomena.

The geometrical structure under consideration is composed of two leads (left and right) plus a central metallic SWNT, with all three parts being metallic SWNT's of the same chirality, which can be described by a tight-binding model with one π electron per atom. The tight-binding Hamiltonian of the system is written as

$$H_C=\sum_i \varepsilon_i a_i^\dagger a_i - V_{pp\pi}\sum_{\langle ij\rangle} a_i^\dagger a_j + \text{c.c.}, \tag{1}$$

where ε_i is the on-site energy, which is taken to have a random distribution, $\varepsilon_i=\varepsilon_0+\Delta\varepsilon_i$ to model the on-site disorder. Here, for simplicity, ε_0 is taken to be zero, and $\Delta\varepsilon_i$ fluctuates between a small interval values $\Delta\varepsilon$. The sum over i,j is restricted to the nearest-neighbor sites, and $V_{pp\pi}=2.75$ eV.[8] Within this formalism, the defect-free nanotubes have complete electron-hole symmetry with their Fermi levels at zero. In our calculations, all nearest-neighbor hopping parameters are assumed to be $V_{pp\pi}$ except those at contacts, which are taken to be $\alpha V_{pp\pi}$ with $0<\alpha<1$. The length of

the central SWNT is taken to be $L=200$ nm(100 nm), which is equivalent to 813(406) layers of carbon atoms for the armchair tubes and 939(470) layers for the zigzag tubes. Consequently, electrons will be slightly scattered at the interfaces for $\alpha \neq 1$ and the system behaves like a Fabry-Perot-type nanotube-electron waveguide.

The conductance G of the SWNT electron waveguide can be calculated by using the Landauer formula $G=(2e^2/h)\mathcal{T}$, with $\mathcal{T}$, the transmission coefficient, which can be expressed as follows:[9,10]

$$\mathcal{T}=\mathrm{Tr}(\Gamma_L G_C^r \Gamma_R G_C^a), \tag{2}$$

where G_C^r and G_C^a are the retarded and advanced Green's functions of the SWNT, respectively, and $\Gamma_L(\Gamma_R)$ is the coupling of the SWNT to the left (right) lead. The Green's function of the SWNT can be explicitly written as

$$G_C(\epsilon)=(\epsilon - H_C - \Sigma_L - \Sigma_R)^{-1}, \tag{3}$$

where $\Sigma_L = h_{LC}^{\dagger} g_L h_{LC}$ and $\Sigma_R = h_{CR} g_R h_{CR}^{\dagger}$ are the self-energy terms due to the semi-infinite leads. h_{LC} and h_{CR} are the coupling matrices with nonzero elements only for the adjacent points between the SWNT and the leads, and $g_{L,R} = (\epsilon - H_{L,R})^{-1}$ are the Green's functions of the two leads. The coupling functions $\Gamma_{L,R}$ can be easily obtained by the following formula:[11]

$$\Gamma_{L,R} = i[\Sigma_{L,R}^r - \Sigma_{L,R}^a]. \tag{4}$$

Following the method in Refs. 6,12, we obtain $\Sigma_L = h_{LC}^{\dagger}\overline{T}$ and $\Sigma_R = h_{CR} T$. Here T and $\overline{T}$ are the appropriate transfer matrices, which are easily computed from the Hamiltonian matrix elements via an iterative procedure:[6,13]

$$T = t_0 + \tilde{t}_0 t_1 + \tilde{t}_0 \tilde{t}_1 t_2 + \cdots + \tilde{t}_0 \tilde{t}_1 \tilde{t}_2, \ldots, t_n + \ldots, \tag{5}$$

$$\overline{T} = \tilde{t}_0 + t_0 \tilde{t}_1 + t_0 t_1 \tilde{t}_2 + \cdots + t_0 t_1 t_2, \ldots, \tilde{t}_n + \ldots, \tag{6}$$

where t_i and $\tilde{t}_i$ are defined via the recursion formulas

$$t_i = (I - t_{i-1}\tilde{t}_{i-1} - \tilde{t}_{i-1} t_{i-1})^{-1} t_{i-1}^2, \tag{7}$$

$$\tilde{t}_i = (I - t_{i-1}\tilde{t}_{i-1} - \tilde{t}_{i-1} t_{i-1})^{-1} \tilde{t}_{i-1}^2, \tag{8}$$

and

$$t_0 = (\epsilon - H_C)^{-1} h_{LC}^{\dagger}, \tag{9}$$

$$\tilde{t}_0 = (\epsilon - H_C)^{-1} h_{CR}. \tag{10}$$

The process is repeated until $t_n, \tilde{t}_n \leqslant \delta$ with δ arbitrarily small.[6,13]

We have calculated the conductance of different metallic SWNT electron resonators at zero temperature and zero bias. Obtained results for the perfect armchair and zigzag SWNTs are shown in Fig. 1, from which it is seen that all metallic SWNT electron resonators can show the slow oscillations except the zigzag ones and the slow oscillation period is inversely proportional to Fermi energy E_F, which is driven by the gate voltage V_g. Also all the metallic SWNT electron resonators exhibit pronounced fast oscillations with the maximum conductance approaching $2G_0$. The fast conductance oscillations period $\Delta E_F \approx 0.0090$ eV for the length $L=200$ nm and $\Delta E_F \approx 0.018$ eV for $L=100$ nm have been obtained, showing its variations proportional to L^{-1} and coinciding very well to the experimental data and the previous theoretical prediction $\Delta E_F = hV_F/2L \approx (1.68\ \mathrm{eV\,nm})/L$.[1,2,6,14] It is the manifestation of electron scattering only at the SWNT-electric contact interface and passing through SWNT ballistically. The ratio of the slow oscillation period to the fast one is independent of the coupling strength between the SWNT and electric contacts, but is relevant to the SWNT length L. All the numerical results said above are well consistent with the analytical result.[6] Since now neither disorder nor defect exists in the central SWNT for Fig. 1, the slow and fast conductance oscillations can only be manifestations of the intrinsic quantum interference in the conducting SWNT's, supporting Jiang *et al.*'s analytical arguments.

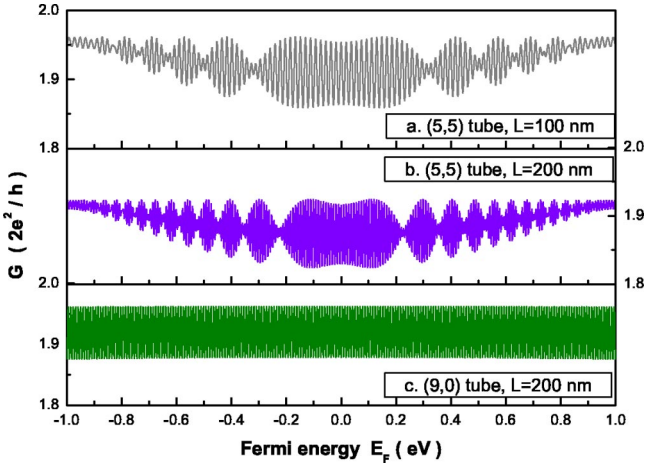

FIG. 1. Conductance G (in unit of G_0) vs Fermi energy E_F for $\alpha=0.70$. (a) (5,5) tube with $L=100$ nm; (b) (5,5) tube, but with $L=200$ nm; (c) (9,0) zigzag tube with $L=200$ nm.

On the other hand, it is found from Figs. 1 and 2 that both the fast and slow oscillations superimpose on a slower variation background, showing more subtle structure in the G vs E_F plot, which is absent in Ref. 6. It is shown that this slower variation background depends on contacts coupling strength and the structure of SWNT. As the contacts coupling is strong (the parameter $\alpha=0.60$, for instance), the SWNT system behaves as electron resonator as seen in Fig. 2(a), but, as the contacts coupling is very weak (e.g., the parameter $\alpha=0.01$), the well-defined resonant peaks appear, showing the limit of conductance oscillations and the resonant transmission. In this case the SWNT system behaves like a quantum dot [as seen in Fig. 2(c)]. At the weaker contacts coupling [$\alpha=0.4$, Fig. 2(b)], as the Fermi energy is driven far from the charge neutrality energy point by the applied gate voltage V_g, the strong contacts-SWNT interfacial scattering makes electrons have the probability to hop to higher subband, leading to decrease of the conductance.[15,16] However, the zigzag-type SWNT electron resonators do not show the slower variation background.

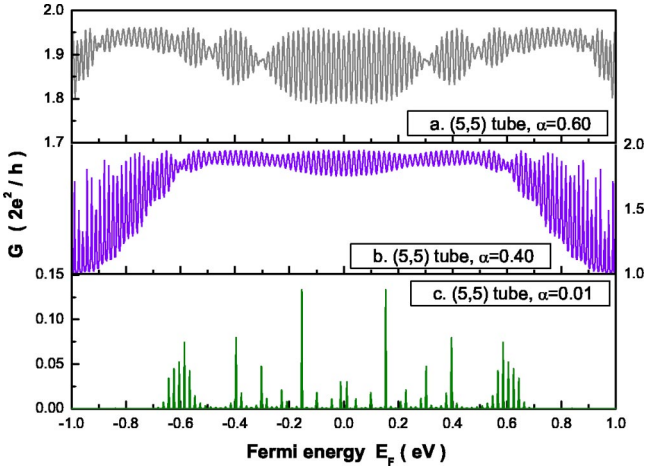

FIG. 2. Conductance G (in unit of G_0) of $L=100$ nm (5,5) tube vs E_F with contact coupling coefficient (a) $\alpha=0.60$; (b) $\alpha=0.40$; (c) $\alpha=0.01$.

Now, let us study the disorder effect on the slow conductance oscillations, which could not be included in the analytical treatment of Ref. 6, but is easily taken into account in our numerical calculations by introducing randomly distributed on-site energies in Eq. (1). The calculated results for the $L=100$ nm (5,5) SWNT with three different degrees of the disorder in the SWNT [$\Delta\varepsilon=0\%$ ($V_{pp\pi}$), 1% ($V_{pp\pi}$), and 3% ($V_{pp\pi}$), respectively] are shown in Fig. 3, from which, it is clearly seen that the slow conductance oscillations can survive in the case of smaller disorder [Fig. 3(b)], but will be smeared out as the disorder becomes larger (Fig. 3(c)], demonstrating the possible disorder in the SWNT disfavors the slow conductance oscillations, and could not be its origin. In order to see more clearly the disorder effect, we have made an amplitude Fourier transformation for the three cases in Fig. 3, and shown the obtained results in Fig. 4. It is clearly seen that in the case of perfect central SWNT [Fig. 4(a)], there are two main frequencies of 55 eV^{-1} and 2.6 eV^{-1}. The main component of 55 eV^{-1} corresponds to the fast

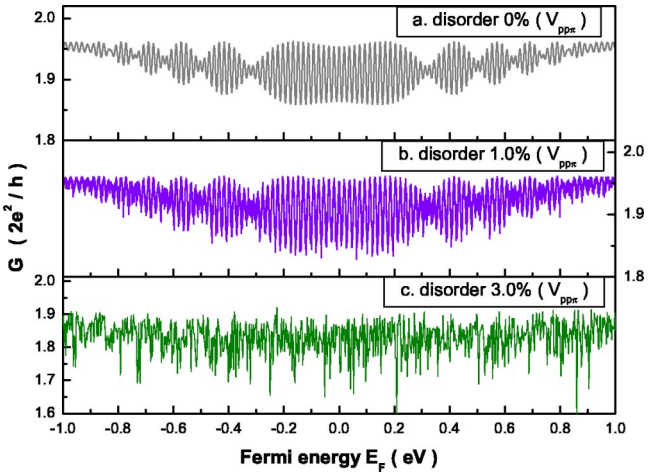

FIG. 3. Conductance G (in unit of G_0) of $L=100$ nm (5,5) tube vs E_F with $\alpha=0.70$, and disorder of (a) 0% ($V_{pp\pi}$); (b) 1% ($V_{pp\pi}$); (c) 3% ($V_{pp\pi}$).

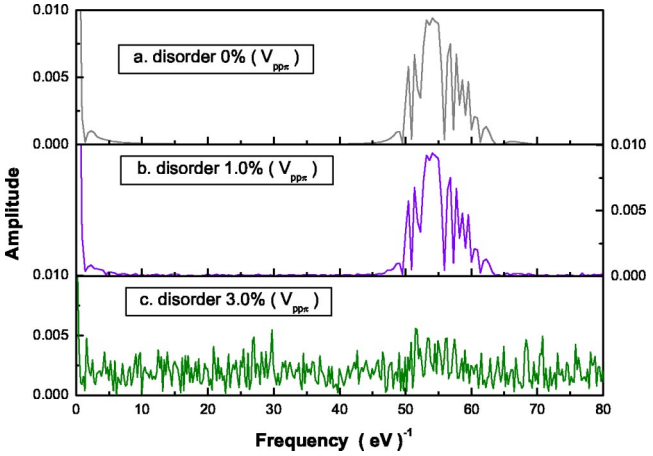

FIG. 4. Amplitude Fourier transformations for three cases of Fig. 3, and disorder of (a) 0% ($V_{pp\pi}$); (b) 1% ($V_{pp\pi}$); (c) 3% ($V_{pp\pi}$).

oscillations and coincides well with previous theoretical prediction value of 59 eV^{-1} for $L=100$ nm SWNT's.[1,2,6,14] The weaker component 2.6 eV^{-1} corresponds to the slow oscillation background. These two main frequencies are weakened in the case of $\Delta\varepsilon=1\%$ ($V_{pp\pi}$) [Fig. 4(b)] and smeared out in the case of $\Delta\varepsilon=3\%$ ($V_{pp\pi}$) [Fig. 4(c)].

Appearance of a deep dip in the conductance oscillation vs the gate voltage plot is an interesting problem, which has not been solved until now. Our numerical calculations show that it probably comes from the chemisorbed atoms on the central SWNT's, which can appear easily in experiments. In our calculations the chemisorbed atom is coupled to one carbon atom of central SWNT for simplicity. Calculations show that its contribution to conductance is to induce a deep dip in the conductance vs E_F plot, being independent of the adsorbed atom position on the SWNT. The width and depth of the deep dip is determined by the coupling strength of the adsorbed atom to SWNT and the position of the deep dip in the conductance curve depends on the on-site energy of the chemisorbed atom. In our calculations the hopping coefficient and the on-site energy for the chemisorbed atom are taken to be $0.2V_{pp\pi}$ (0.55 eV) and $0.11V_{pp\pi}$ (0.30 eV), respectively, to fit the experimental data, and obtained result is shown in Fig. 5(a), from which it is clearly seen that a deep dip appears at $0.11V_{pp\pi}$ (0.30 eV) with the fast conductance superimposed on it. We have also calculated the system with five chemisorbed atoms, which have the same hopping coefficient and different on-site energies in one case [Fig. 5(b)], as well as the same on-site energy and different hopping coefficients in another case [Fig. 5(c)]. It seems that Fig. 5(b) is more like that observed in experiment.[2] All the obtained results clearly show that the chemisorbed atoms could be an origin of the deep conductance dip in the G vs E_F curve, observed in experiment.

On the other hand, it is well known that the specific topological defects in the SWNT's have big effects on the transport properties of the SWNT.[17] So, it is natural to ask whether or not they can be the origin of the slow conductance oscillations or the deep dip. We have calculated the conductance of (5,5) SWNT with a pentagon-heptagon (5-7-

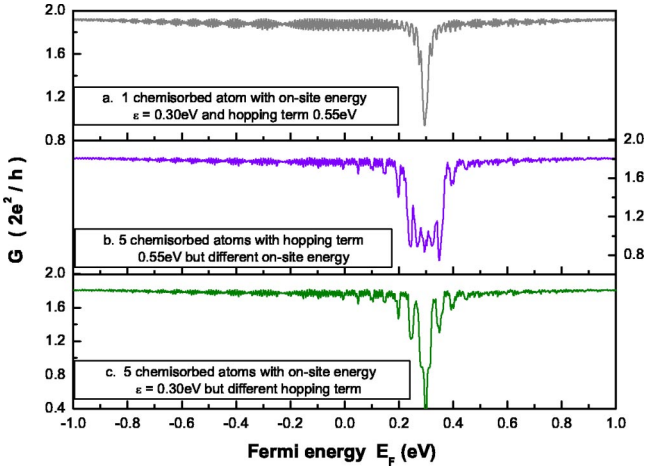

FIG. 5. Conductance G (in unit of G_0) of $L=200$ nm (5,5) tube vs E_F with $\alpha=0.70$. (a) One chemisorbed atom of on-site energy 0.30 eV and hopping coefficient 0.55 eV; (b) five chemisorbed atoms with the same hopping coefficient of 0.55 eV and different on-site energies of 0.25 eV, 0.28 eV, 0.30 eV, 0.33 eV, and 0.36 eV, respectively. (c) Five chemisorbed atoms with the same on-site energy of 0.30 eV and different hopping coefficients of 0.40 eV, 0.50 eV, 0.55 eV, 0.60 eV, and 0.70 eV, respectively.

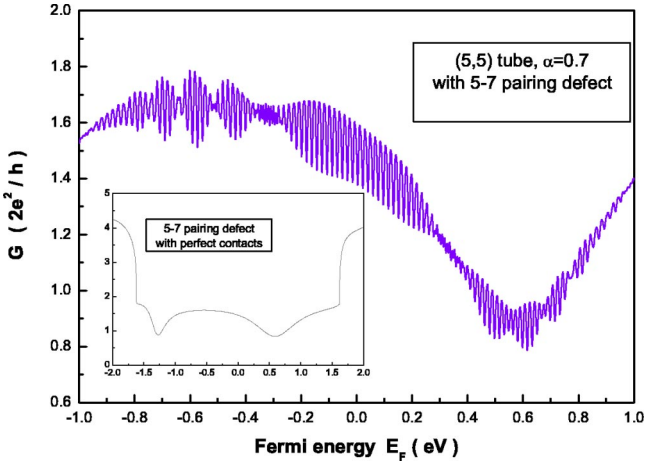

FIG. 6. Conductance G (in unit of G_0) of $L=200$ nm (5,5) tube vs E_F with $\alpha=0.70$ and one pentagon-heptagon pair. Inset: the conductance of the same resonator but with perfect contacts.

7-5) pair on it, and the obtained result is shown in Fig. 6, in which, for comparison, the system conductance with perfect contacts is also given. It is seen that even in the case of perfect contacts, the 5-7-7-5 defects can induce two conductance dips, distributed below and above the Fermi level, respectively, but there are no fast and slow conductance oscillations. When the interfacial scattering is added (e.g., α is taken to be 0.7), both the fast and slow conductance fluctuations appear and are superimposed on the dips, but the dips seem to be too wide and shallow in contrast to the experimental observations. So, the topological defects could not be the origin of the slow conductance oscillations, and the deep dip either.

In conclusion, our numerical calculations demonstrate that all metallic SWNT resonators, except the zigzag ones, have the slow conductance oscillations at strong contact coupling, and show well-defined resonant peaks as the coupling becomes very weak, which are the manifestation of the intrinsic quantum interference in the SWNT resonator. More importantly, it is found that the deep dip in the $G\sim E_F$ curve can be ascribed to the chemisorbed atom on the central SWNT of the resonator, which, however, cannot cause the fast and slow conductance oscillations. The disorder and the topological defect cannot do it either. Our results provide a consistent explanation for the observed phenomena.

This work was supported by the Natural Science Foundation of China under Grant Nos. 10074026 and A040108. The authors acknowledge also support from a Grant for State Key Program of China through Grant No. 1998061407.

[1] W. Liang *et al.*, Nature (London) **411**, 665 (2001).
[2] J. Kong *et al.*, Phys. Rev. Lett. **87**, 106801 (2001).
[3] A. Bachtold *et al.*, Phys. Rev. Lett. **84**, 6082 (2000).
[4] H. Soh *et al.*, Appl. Phys. Lett. **75**, 627 (1999).
[5] J. Nygard *et al.*, Nature (London) **408**, 342 (2000).
[6] J. Jiang, J. Dong, and D.Y. Xing, Phys. Rev. Lett. **91**, 056802 (2003).
[7] M.B. Nardelli, Phys. Rev. B **60**, 7828 (1999).
[8] L. Chico *et al.*, Phys. Rev. Lett. **76**, 971 (1996).
[9] D.S. Fisher and P.A. Lee, Phys. Rev. B **23**, 6851 (1981).
[10] Y. Meir and N.S. Wingreen, Phys. Rev. Lett. **68**, 2512 (1992).
[11] S. Datta, *Electronic Transport in Mesoscopic Systems* (Cambridge University Press, Cambridge, 1995).
[12] F. Garcia-Moliner *et al.*, Phys. Rep. **200**, 83 (1991).
[13] M.P. Lopez-Sancho *et al.*, J. Phys. F: Met. Phys. **14**, 1205 (1984); **15**, 851 (1985).
[14] A. Rubio *et al.*, Phys. Rev. Lett. **82**, 3520 (1999).
[15] P.F. Bagwell, Phys. Rev. B **41**, 10 354 (1990).
[16] E. Tekman and S. Ciraci, Phys. Rev. B **42**, 9098 (1990).
[17] D. Orlikowski *et al.*, Phys. Rev. B **63**, 155412 (2001).